

**European summer  
surface ozone  
1990–2100**

J. Langner et al.

# European summer surface ozone 1990–2100

**J. Langner, M. Engardt, and C. Andersson**

Swedish Meteorological and Hydrological Institute, 60176, Norrköping, Sweden

Received: 28 February 2012 – Accepted: 6 March 2012 – Published: 16 March 2012

Correspondence to: J. Langner (joakim.langner@smhi.se)

Published by Copernicus Publications on behalf of the European Geosciences Union.

Title Page

Abstract

Introduction

Conclusions

References

Tables

Figures

◀

▶

◀

▶

Back

Close

Full Screen / Esc

Printer-friendly Version

Interactive Discussion



## Abstract

The impact of climate change and changes in ozone precursor emissions on summer surface ozone in Europe were studied using a regional CTM over the period 1990 to 2100. Two different climate simulations under the SRES A1B scenario together with ozone precursor emission changes from the RCP4.5 scenario were used as model input. In southern Europe regional climate change leads to increasing surface ozone concentrations during April–September, but projected emission reductions in Europe have a stronger effect, resulting in net reductions of surface ozone concentrations. In northern Europe regional climate change decreases surface O<sub>3</sub> and reduced emissions acts to further strengthen this trend also when including increasing hemispheric background concentrations, although on the British Isles the combined effect is an increase. Due to substantial decadal variability in the simulations it is important to study averages over sufficiently long time periods in order to be able to extract robust signals of climate change impacts on surface O<sub>3</sub> concentrations.

## 1 Introduction

Surface ozone (O<sub>3</sub>) has negative effects on human health and vegetation. Background levels of O<sub>3</sub> in the lower troposphere over the northern mid-latitudes have increased by a factor of two to three since the end of the 19th century (Parrish et al., 2009). This is to a large extent related to increasing man made emissions of O<sub>3</sub> precursors such as methane (CH<sub>4</sub>), carbon monoxide (CO), nitrogen oxides (NO<sub>x</sub>) and non-methane volatile organic compounds (NMVOC) (Isaksen et al., 2009). O<sub>3</sub> in the lower troposphere is also regulated by climatic factors such as temperature and solar radiation as well as by surface deposition which in the case of vegetated surfaces is again regulated by temperature, solar radiation, humidity and soil water availability (Jacob and Winner, 2009; Andersson and Engardt, 2010). Given that projections of future climate in Europe indicate substantial changes in these variables there is concern about increasing concentrations of O<sub>3</sub> due to climate change (Royal Society, 2008).

## European summer surface ozone 1990–2100

J. Langner et al.

Title Page

Abstract

Introduction

Conclusions

References

Tables

Figures

◀

▶

◀

▶

Back

Close

Full Screen / Esc

Printer-friendly Version

Interactive Discussion



---

**European summer  
surface ozone  
1990–2100**

---

J. Langner et al.

---

[Title Page](#)[Abstract](#)[Introduction](#)[Conclusions](#)[References](#)[Tables](#)[Figures](#)[⏪](#)[⏩](#)[◀](#)[▶](#)[Back](#)[Close](#)[Full Screen / Esc](#)[Printer-friendly Version](#)[Interactive Discussion](#)

Several studies with regional chemistry transport models have pointed out the importance of climate change for future surface  $O_3$  in Europe (e.g. Langner et al., 2005; Meleux et al., 2007; Engardt et al., 2009; Andersson and Engardt, 2010; Katragku et al., 2011). The previous studies based their analysis on simulations over time slices of 10–30 yr for current and future climate. In most cases climate projections based on one global climate model was used. The purpose of the present study is to extend the analysis of future changes in surface  $O_3$  in Europe to include the combined transient effects of changes in climate, changes in  $O_3$  precursor emissions and changes in background concentrations over the 110-yr period from 1990 to 2100. We use recent compilations of historic and future trends of emissions of air pollutants over Europe and climate projections from two different global climate models downscaled over Europe to provide regional detail.

Section 2 provides details on the setup of the current study including general information on the utilized climate and chemistry transport models. Section 2 also contains an evaluation of the modelling systems' ability to reproduce surface  $O_3$  concentrations in Europe. In Sect. 3 we present the results. We focus on summer (April–September) mean and mean of daily maximum (daily max) concentrations of  $O_3$ . This is the main growing season and surface  $O_3$  is at its maximum in Europe and hence this period is of main interest for impacts on human health and vegetation. Finally we present conclusions in Sect. 4.

## 2 Methods and data

To simulate the evolution of surface ozone over Europe during the period 1990–2100 we make use of a chain of models starting with global climate models (GCMs) that feeds boundary conditions into a regional climate model (RCM) with higher spatial resolution over Europe. The resulting meteorological output from the RCM is then used to drive the simulation of emissions, transport, atmospheric chemistry and deposition of air pollutants in a chemistry transport model (CTM) over Europe.

## 2.1 Climate projection

In order to investigate the uncertainty related to the choice of GCM in projecting future climate change we used results downscaled by a RCM from two different GCMs; the ECHAM5 model (Roeckner et al., 2006) and the HadCM3 model (Collins et al., 2011).

5 The RCM used was the Rossby Centre Regional Climate model version 3, RCA3. Model description and evaluation of both current and future climate simulated with RCA3 is given by Samuelsson et al. (2011) and Kjellström et al. (2011). Both climate projections used in this study were derived using the SRES A1B scenario (Nakićenović et al., 2000). Six-hourly meteorological output on 21 model levels, as well as a range  
10 of output variables at the surface, was stored from the RCA3 simulations to be used in the CTM modelling. The climate as downscaled by RCA3 carries on broad features of the climate simulated by the parent GCM. The projection downscaled from HadCM3 has an average temperature change of 2.9 °C between the periods 1961–1990 and 2040–2070 for the European domain while the corresponding value for the projection  
15 downscaled from ECHAM5 is 2.0 °C. The HadCM3 projection thereby has the second highest temperature change in an ensemble of 16 different projections downscaled from different GCM runs by RCA3 over Europe while the ECHAM5 projection has the fourth lowest (Kjellström et al., 2011). Apart from differences in mean temperature change there are other differences between the two projections on the regional scale  
20 within Europe. In particular the reduction of precipitation in summer is larger in south-western Europe in ECHAM5 and consequently also cloud cover and soil moisture. These factors are important for ozone production and dry deposition to vegetation.

## 2.2 Regional chemistry transport model

We used the regional, off-line, Eulerian CTM, MATCH, to simulate the evolution of O<sub>3</sub> and a range of other air pollutants over Europe. The model structure, boundary layer  
25 parameterization, advection scheme and numerical treatment are given by Robertson et al. (1999). The chemical scheme in MATCH is based on Simpson et al. (1993),

Title Page

Abstract

Introduction

Conclusions

References

Tables

Figures

◀

▶

◀

▶

Back

Close

Full Screen / Esc

Printer-friendly Version

Interactive Discussion



---

**European summer  
surface ozone  
1990–2100**J. Langner et al.

---

[Title Page](#)[Abstract](#)[Introduction](#)[Conclusions](#)[References](#)[Tables](#)[Figures](#)[⏪](#)[⏩](#)[◀](#)[▶](#)[Back](#)[Close](#)[Full Screen / Esc](#)[Printer-friendly Version](#)[Interactive Discussion](#)

with extensions described by Andersson et al. (2007). The dry deposition of gases and aerosols is calculated using a resistance approach depending on land surface type and for gases the deposition to vegetated surfaces is coupled to soil moisture, temperature, vapour pressure deficit and photosynthetically active radiation (PAR) as described in Andersson and Engardt (2010). The wet scavenging is assumed to be proportional to the precipitation intensity for most gaseous and aerosol components. For O<sub>3</sub>, hydrogen peroxide and sulfur dioxide in-cloud scavenging is calculated assuming Henry's law equilibrium; sub-cloud scavenging is neglected for these species. Important model parameters, such as dry deposition velocities and scavenging coefficients are tabulated in Andersson et al. (2007). The model domain covers Europe and part of the North Atlantic using a rotated latitude-longitude grid with 85 by 95 cells and a horizontal resolution of 0.44° by 0.44° (ca. 50 by 50 km). In the vertical direction, the CTM domain reaches 5–6 km above the surface using 15 model levels. The lowest model layer is ~60 m thick, increasing to ~700 m in layer 15. The temporal resolution of the meteorological input data is six hours, interpolated to one hour in MATCH; the overall model time step is ten minutes.

### 2.3 Emission data

Anthropogenic emissions of NO<sub>x</sub>, sulfur dioxide, ammonia, NMVOC and CO used in the MATCH simulations were taken from the RCP4.5 scenario (Thomson et al., 2011; Lamarque et al., 2010). The RCP scenarios have been developed as a replacement of the SRES scenarios and are now the basis for current modelling activities in the climate modelling community. There are four RCP scenarios corresponding to total anthropogenic radiative forcing estimated to 2.6, 4.5, 6 and 8.5 W m<sup>-2</sup> respectively in the year 2100. The RCP data base provides global gridded historic anthropogenic emissions and scenarios for future emissions for different sectors and pollutants on a 0.5° by 0.5° latitude-longitude grid. Emission estimates are available for every ten years and for use in the CTM modelling we linearly interpolated this data to yearly resolution. In the RCP4.5 scenario anthropogenic ozone precursor emissions decrease substantially

in Europe: NO<sub>x</sub>, NMVOC and CO emissions decrease by 53, 22 and 17 % respectively, from year 2000 to 2050, for the domain covered by the CTM simulations.

Emissions of biogenic isoprene are calculated online in MATCH following Simpson et al. (1995). The isoprene source strength is a function of vegetation type (i.e. tree species), local temperature and PAR. The calculated isoprene emissions increase with PAR and temperature, which are from the driving regional climate model. The relative proportion of the different tree species in each grid cell remains the same throughout all model scenarios. There is currently no treatment of natural sources of nitrogen in MATCH.

## 2.4 Boundary conditions

Boundary conditions of the chemical components simulated by MATCH were held at current levels (ca. year 2000) in the simulations with a monthly, horizontal and vertical variation as described in Andersson et al. (2007). Concentrations of O<sub>3</sub> at background locations in Europe have been increasing during the last few decades (Lelieveld et al., 2004; Derwent et al., 2007) although the observed trend has weakened in the first years of the 21st century. A similar increase is also observed in the boundary layer air inflow at the west coast of North America (Parrish et al., 2009). To assess the importance of continued increase of background O<sub>3</sub> we performed one simulation where the background concentration of O<sub>3</sub> increase by 0.1 ppbv yr<sup>-1</sup> from 1990 to 2100. This is a weaker trend than has been observed during recent decades at Mace Head (Derwent et al., 2007) but still implies a substantial increase of background O<sub>3</sub> of 5 ppbv over the period 2000–2050. In this experiment we also allow the concentration of CH<sub>4</sub> to vary according to the concentration pathway provided by the RCP4.5 scenario. This means that the global average concentration of CH<sub>4</sub> increases to a maximum of 1842 ppbv in 2040 and then drops to 1576 ppbv in 2100.

## European summer surface ozone 1990–2100

J. Langner et al.

Title Page

Abstract

Introduction

Conclusions

References

Tables

Figures

◀

▶

◀

▶

Back

Close

Full Screen / Esc

Printer-friendly Version

Interactive Discussion



## 2.5 Model evaluation

To evaluate the performance of the MATCH-RCA3 modelling system, we compare our “Increasing boundary case” (see below) to measured O<sub>3</sub> concentrations for 1990–2009. The observations were extracted from the EBAS data base (<http://ebas.nilu.no>).

5 The results of the evaluation are displayed in Table 1. The O<sub>3</sub> measures compared are daily mean and daily maximum averages, for the summer half year for stations north and south of 50° N respectively. The present setup of the modelling system shows comparable performance as earlier applications of MATCH using climate model output (e.g. Langner et al., 2005; Andersson and Engardt, 2010), but the spatial correlation is not as good. Part of the difference can be related to the differences in climate simulated by the versions of the GCMs used in the different studies. Evaluation of MATCH driven by meteorological data constrained by observations shows better correlation (e.g. van Loon et al., 2007). Emission data also impacts the results and the comparison is sensitive to which simulated time period that is used in the comparison, due to long-term (decadal) variations in the simulated climate that do not necessarily coincide with the observed meteorology. The spatial correlation for average ozone north of 50° N is particularly low while it is higher to the south and also higher for average of daily maximum. The bias and RMSE for mean O<sub>3</sub> in north Europe is comparable to the values in south Europe and for mean of daily maximum. The low spatial correlation for average ozone in the north could partly be due to biases in the simulation of current climate in the global climate projection from ECHAM5. The simulated current climate in summer over northern Europe in ECHAM5 is too cold and wet (Kjellström et al., 2011).

## 3 Results and discussion

In this section we discuss the results from four MATCH simulations covering the period 1990–2100:

### European summer surface ozone 1990–2100

J. Langner et al.

Title Page

Abstract

Introduction

Conclusions

References

Tables

Figures



Back

Close

Full Screen / Esc

Printer-friendly Version

Interactive Discussion



**European summer  
surface ozone  
1990–2100**

J. Langner et al.

Title Page

Abstract

Introduction

Conclusions

References

Tables

Figures

◀

▶

◀

▶

Back

Close

Full Screen / Esc

Printer-friendly Version

Interactive Discussion

1. Climate sensitivity case 1 (ECH\_RCP2000\_BC2000); describing the effect of changing climate (downscaled ECHAM5) on surface  $O_3$ . Boundary concentration of  $CH_4$  and  $O_3$ , and anthropogenic precursor emissions are kept at the level of year 2000.
2. Climate sensitivity case 2 (HAD\_RCP2000\_BC2000); modelling set up as in case 1, but simulated with another climate projection (downscaled HadCM3).
3. Emission reduction case (ECH\_RCP4.5\_BC2000); where anthropogenic  $O_3$  precursor emissions in Europe follow RCP4.5, while background concentrations of  $O_3$  and  $CH_4$  are kept at the level of year 2000. The climate projection downscaled from ECHAM5 is used in this case.
4. Increasing boundary case (ECH\_RCP4.5\_BCtrend); including varying anthropogenic precursor emissions in Europe according to RCP4.5, increasing background ozone with  $0.1 \text{ ppbv yr}^{-1}$  and changing  $CH_4$  concentrations following RCP4.5. The climate projection downscaled from ECHAM5 is used in this case.

Figure 1a and b shows results for the temporal evolution of summer mean and summer mean of daily max  $O_3$  for the four simulations averaged over the European land area north and south of  $50^\circ \text{ N}$ , respectively.

The upper two lines in each four-line group correspond to the two climate sensitivity cases (ECH\_RCP2000\_BC2000 and HAD\_RCP2000\_BC2000). Here we kept the  $O_3$  precursor emissions and boundary concentrations constant over time at their year 2000 values to isolate the effect of meteorological changes. For northern Europe we note a slight downward trend for daily max ( $-0.5$  and  $-0.8 \text{ ppbv century}^{-1}$  for ECH\_RCP2000\_BC2000 and HAD\_RCP2000\_BC2000 respectively) with small inter-annual variability. Trends over the whole period are given in Table 2. In southern Europe there is an increase in surface  $O_3$  over time for the climate sensitivity cases. The variability in the simulations are different for different time periods, but the trends in the two simulations are similar ( $+3.5$  and  $+3.2 \text{ ppbv century}^{-1}$  for daily max). Earlier

studies using the MATCH model have shown that two main drivers for the increasing summer surface  $O_3$  in southern Europe are decrease in dry deposition of  $O_3$  due to reduced soil water and thereby reduced vegetation uptake, and increase in biogenic isoprene emissions, with decrease in dry deposition being the dominant effect in the southern-most parts of Europe and both being equally important in central Europe (Andersson and Engardt, 2010). It is interesting to note the substantial decadal variability in the trend of surface  $O_3$  especially in southern Europe. For example, during the period 2020 to 2030 climate variability leads to decreasing surface  $O_3$  in southern Europe in both the ECH\_RCP2000\_BC2000 and HAD\_RCP2000\_BC2000 simulation, with a more prominent decrease in the latter case.

When we include also the change in ozone precursor emissions in Europe following the RCP4.5 scenario (ECH\_RCP4.5\_BC2000) we obtain decreasing surface  $O_3$  concentrations across Europe. The impact of reduced emissions in Europe clearly dominates over climate change impacts and leads to reductions of daily max  $O_3$  both in northern and southern Europe until 2100 ( $-9.2$  and  $-12.8$  ppbv century $^{-1}$ , respectively). Applying a potential trend of background  $O_3$  of  $+0.1$  ppbv yr $^{-1}$  (ECH\_RCP4.5\_BCtrend) results in partial cancellation of the  $O_3$  decrease due to emission changes in – especially northern – but also southern Europe. The resulting change in surface  $O_3$  from 1990 to 2100 in these regions now become  $-5.0$  and  $-9.7$  ppbv century $^{-1}$ , respectively.

Due to substantial year to year variability in the simulations it is important to study averages over sufficiently long time periods in order to be able to extract robust signals. We use climate projections from two global climate models to account for some of the uncertainty in simulating future climate change. Although the long-term trend in the two simulations is similar, differences for shorter periods can be large as a reflection of the inherent variability in the climate system. Table 2 summarizes 20-yr average concentrations and variability for northern and southern Europe over the periods 1990–2009, 2040–2059 and 2080–2099. The absolute variability is larger in southern Europe than in northern and it increases with time in the climate sensitivity case based on

**European summer  
surface ozone  
1990–2100**

J. Langner et al.

Title Page

Abstract

Introduction

Conclusions

References

Tables

Figures

◀

▶

◀

▶

Back

Close

Full Screen / Esc

Printer-friendly Version

Interactive Discussion



ECHAM5. When using HadCM3 the variability first increases and then decreases. The opposite is seen in the Emission reduction case and Increasing boundary case. The decrease until mid-century is probably due to decreasing emissions whereas the increasing variability in the ECHAM5 downscaling cause further variability beyond this point as can be seen throughout the century in the ECH\_RCP2000\_BC2000 case.

Figure 2 shows the current and future frequency distributions of O<sub>3</sub> concentrations in northern and southern Europe for the Increasing boundary case. Here we observe that there is a shift of the peak of the distribution to lower concentrations, the shift being slightly smaller for northern Europe than for southern Europe. For high concentrations we note larger changes in the frequency distribution both in northern and southern Europe. This shows that emission reductions within Europe are especially effective in reducing the highest O<sub>3</sub> concentrations connected to O<sub>3</sub> episodes also in northern Europe although the overall average is only reduced slightly due to increasing background concentrations.

The spatial distributions of the changes in mean and daily max O<sub>3</sub> between the periods 1990–2009 and 2040–2059 for the four simulations are shown in Figs. 3 and 4 respectively. Climate change alone increases O<sub>3</sub> in southern Europe in both the climate sensitivity simulations. The increase is generally in the range 0–3 ppbv for summer mean. Decrease of 0–3 ppbv in summer mean O<sub>3</sub> is simulated in the northern part of the model domain. Changes for summer mean of daily max are somewhat larger, 3–6 ppbv, in regions of southern Europe, while there are reductions in the northern part of the model domain in the range 0–3 ppbv. Increases are somewhat larger when using the HadCM3 projection and also cover larger areas of Europe. When including the trend in RCP4.5 anthropogenic precursor emissions, reductions of O<sub>3</sub> are evident everywhere except in northern Africa where O<sub>3</sub> precursor emissions are increasing until 2040 in RCP4.5 and for a few grid points close to Helsinki and Moscow. In these urban areas the reductions in NO<sub>x</sub> emissions lead to a reduced loss of O<sub>3</sub> through reaction with NO and increasing O<sub>3</sub> concentrations locally. For mean O<sub>3</sub> the effect is visible also for a few other locations in the northern part of Europe, e.g. London and

**European summer  
surface ozone  
1990–2100**

J. Langner et al.

Title Page

Abstract

Introduction

Conclusions

References

Tables

Figures

◀

▶

◀

▶

Back

Close

Full Screen / Esc

Printer-friendly Version

Interactive Discussion



Amsterdam while the effect is not visible further south. This is related to differences in photochemical regimes in different parts of Europe with more NO<sub>x</sub> sensitive regimes in northern Europe (Beekman and Vautard, 2010). Reductions exceed 9 ppbv for summer mean and 12 ppbv for summer daily max in a region extending from northern Italy to Hungary. For the Increasing boundary case the assumed upward trend in background O<sub>3</sub> clearly impacts the concentration along the western and northern part of the model domain. The change over the North Atlantic and the British Isles is reversed from negative to positive compared to the scenario with constant boundaries, with net O<sub>3</sub> changes now of 0 to +3 ppbv on the British Isles for daily mean. However, most parts of the European land areas still experiences decreasing mean O<sub>3</sub>. Corresponding changes in daily max O<sub>3</sub> have a similar geographical pattern, but smaller magnitude.

It is clear from the results presented above that the future evolution of background tropospheric O<sub>3</sub> in the Northern Hemisphere will be important for the resulting surface O<sub>3</sub> concentration in large parts of Europe. Isaksen et al. (2009) reviewed global model studies looking at the impact of future changes in O<sub>3</sub> precursor emissions. Under a SRES A2 scenario surface O<sub>3</sub> concentrations in 2030 could increase by 4–6 ppbv around Europe, in line with our Increasing boundary case, and would then continue to increase until 2100 (Prather et al., 2003). On the other hand a SRES B2 scenario plus additional measures targeted at O<sub>3</sub> precursors could result in reductions of O<sub>3</sub> concentrations around Europe. Wild et al. (2012) present estimates of regional changes of surface O<sub>3</sub> based on average source receptor calculations with 14 different global models for present (2001) meteorological conditions. They estimate that changes in annual mean O<sub>3</sub> between 2000 and 2050 averaged over Europe would be negative for all RCP scenarios except for RCP 8.5 which has the largest increase of greenhouse gases. The changes are substantially different than estimated with the SRES A1B, A2 and B2 scenarios, reflecting the assumptions of more stringent O<sub>3</sub> precursor emission controls under the RCP scenarios. Domain and annual average changes in mean O<sub>3</sub> between the 20-yr periods 1990–2009 and 2040–2059 in our Increasing boundary case is –0.2 ppbv which can be compared to –2.7 and +0.3 ppbv estimated by Wild

**European summer  
surface ozone  
1990–2100**

J. Langner et al.

Title Page

Abstract

Introduction

Conclusions

References

Tables

Figures

◀

▶

◀

▶

Back

Close

Full Screen / Esc

Printer-friendly Version

Interactive Discussion



et al. (2012) for RCP4.5 and 8.5 respectively. The domain average change in annual mean  $O_3$  from 1990–2009 to 2040–2059 in our Emission reduction case, which assumes that background  $O_3$  is unchanged around Europe, is  $-2.5$  ppbv which is similar to the total change given by Wild et al. (2012) for RCP 4.5 but it is somewhat larger than the change they estimate due to reduction in European precursor emissions for RCP 8.5 and 2.6, which are about  $-1.5$  to  $-2$  ppbv. It should be noted that the European domains used in these calculations are not identical; the domain used by Wild et al. (2012) being larger and shifted to the east and south. For the summer period the decrease in domain averaged mean values from 1990–2009 to 2040–2059 is much larger,  $-2.4$  and  $-4.3$  ppbv for our Increasing boundary case and Emission reduction case respectively, illustrating that the reduction in European  $O_3$  precursor emissions are much more important in summer than in the annual mean.

## 4 Conclusions

We have studied the impact of climate change and changes in  $O_3$  precursor emissions on summer time surface  $O_3$  over Europe using two different projections of global climate from the SRES A1B scenario and the combined effect of also including ozone precursor emission changes under the RCP4.5 scenario over the period 1990 to 2100. The following conclusions can be drawn:

1. The MATCH CTM simulations using climate model output are able to capture major features of the observed distribution of surface  $O_3$  over Europe although the spatial correlation is lower compared to simulations using meteorological data constrained by observations.
2. In southern Europe regional climate change gives a substantial positive contribution to future surface  $O_3$  concentrations, but emission reductions are more important leading to reduced  $O_3$  concentrations, also when including increasing hemispheric background concentrations.

## European summer surface ozone 1990–2100

J. Langner et al.

Title Page

Abstract

Introduction

Conclusions

References

Tables

Figures

◀

▶

◀

▶

Back

Close

Full Screen / Esc

Printer-friendly Version

Interactive Discussion



**European summer  
surface ozone  
1990–2100**

J. Langner et al.

[Title Page](#)[Abstract](#)[Introduction](#)[Conclusions](#)[References](#)[Tables](#)[Figures](#)[◀](#)[▶](#)[◀](#)[▶](#)[Back](#)[Close](#)[Full Screen / Esc](#)[Printer-friendly Version](#)[Interactive Discussion](#)

3. In northern Europe regional climate change decreases surface  $O_3$  and reduced emissions acts to further strengthen this trend also when including increasing hemispheric background concentrations, although on the British Isles the combined effect is an increase.

5 4. The sensitivity to regional climate change using climate projections from two global climate models gave similar spatial changes in surface  $O_3$  and similar long-term temporal trends although the trends differ between different periods.

10 5. Due to substantial decadal variability in the simulations it is important to study averages over sufficiently long time periods in order to be able to extract robust signals of climate change impacts on surface  $O_3$  concentrations.

In this study we have used a regional CTM coupled to a regional climate model to simulate details in changes of surface  $O_3$  over Europe over long time periods. A drawback with this model setup is that assumptions have to be made about trends in the concentrations of chemical components on the model boundaries. Ultimately the spatial  
15 resolution of global CTMs will be adequate to simulate also regional details of surface  $O_3$ . Until then coupling of global (hemispheric) and regional CTMs forced by a consistent set of meteorological data and precursor emissions is a useful way forward.

*Acknowledgements.* This study was supported by Swedish Environmental Protection Agency through the research programme CLEO – Climate Change and Environmental Objectives and the European Union seventh framework research program projects ECLAIRE (project  
20 no: 282910) and SUDPLAN (project no: 247708). Climate model output was delivered by the Rossby Centre at the Swedish Meteorological and Hydrological Institute.

## References

- Andersson, C. and Engardt, M.: European ozone in a future climate – The importance of changes in dry deposition and isoprene emissions, *J. Geophys. Res.*, 115, D02303, doi:10.1029/2008JD011690, 2010.
- 5 Andersson, C., Langner, J., and Bergström, R.: Interannual variation and trends in air pollution over Europe due to climate variability during 1958-2001 simulated with a regional CTM coupled to the ERA40 reanalysis, *Tellus B*, 59, 77–98, 2007.
- Beekmann, M. and Vautard, R.: A modelling study of photochemical regimes over Europe: robustness and variability, *Atmos. Chem. Phys.*, 10, 10067–10084, doi:10.5194/acp-10-10067-10, 2010.
- 10 Collins, M., Booth, B. B. B., Bhaskaran, B., Harris, G. R., Murphy, J. M., Sexton, D. M. H., and Webb, M. J.: Climate model errors, feedbacks and forcings: a comparison of perturbed physics and multi-model ensembles, *Clim. Dynam.*, 36, 1737–1766, doi:10.1007/s00382-010-0808-0, 2011.
- 15 Derwent, R. G., Simmonds, P. G., Manning, A. J., and Spain, T. G.: Trends over a 20-year period from 1987 to 2007 in surface ozone at the atmospheric research station, Mace Head, Ireland, *Atmos. Environ.*, 41, 9091–9098, 2007.
- Engardt, M., Bergström, R., and Andersson, C.: Climate and emission changes contributing to changes in near-surface ozone in Europe over the coming decades: Results from model studies, *Ambio*, 38, 452–458, 2009.
- 20 Isaksen, I. S. A., Granier, C., Myhre, G., Berntsen, T. K., Dalsøren, S. B., Gauss, M., Klimont, Z., Benestad, R., Bousquet, P., Collins, W., Cox, T., Eyring, V., Fowler, D., Fuzzi, S., Jöckel, P., Laj, P., Lohmann, U., Maione, M., Monks, P., Prevo, A. S. H., Raes, F., Richter, A., Rognerud, B., Schulz, M., Shindell, D., Stevenson, D. S., Storelvmo, T., Wang, W.-C., van Weele, M., Wild, M., and Wuebbles, D.: Atmospheric Composition Change: Climate-Chemistry interactions, *Atmos. Environ.*, 43, 5138–5192, 2009.
- 25 Jacob, D. J. and Winner, D. A.: Effect of climate change on air quality, *Atmos. Environ.*, 43, 51–63, 2009.
- Katragkou, E., Zanis, P., Kioutsioukis, I., Tegoulas, I., Melas, D., Krüger, B. C., and Coppola, E.: Future climate change impacts on summer surface ozone from regional climate-air quality simulations over Europe, *J. Geophys. Res.*, 116, D22307, doi:10.1029/2011JD015899, 2011.
- 30

### European summer surface ozone 1990–2100

J. Langner et al.

Title Page

Abstract

Introduction

Conclusions

References

Tables

Figures

◀

▶

◀

▶

Back

Close

Full Screen / Esc

Printer-friendly Version

Interactive Discussion



## European summer surface ozone 1990–2100

J. Langner et al.

Title Page

Abstract

Introduction

Conclusions

References

Tables

Figures

◀

▶

◀

▶

Back

Close

Full Screen / Esc

Printer-friendly Version

Interactive Discussion



Kjellström, E., Nikulin, G., Hansson, U., Strandberg, G., and Ullerstig, A.: 21st century changes in the European climate: uncertainties derived from an ensemble of regional climate model simulations, *Tellus A*, 63, 24–40, doi:10.1111/j.1600-0870.2010.00475.x, 2011.

Lamarque, J.-F., Bond, T. C., Eyring, V., Granier, C., Heil, A., Klimont, Z., Lee, D., Liousse, C., Mieville, A., Owen, B., Schultz, M. G., Shindell, D., Smith, S. J., Stehfest, E., Van Aardenne, J., Cooper, O. R., Kainuma, M., Mahowald, N., McConnell, J. R., Naik, V., Riahi, K., and van Vuuren, D. P.: Historical (1850–2000) gridded anthropogenic and biomass burning emissions of reactive gases and aerosols: methodology and application, *Atmos. Chem. Phys.*, 10, 7017–7039, doi:10.5194/acp-10-7017-2010, 2010.

Langner, J., Bergström, R., and Foltescu, V.: Impact of climate change on surface ozone and deposition of sulphur and nitrogen in Europe, *Atmos. Environ.*, 39, 1129–1141, 2005.

Lelieveld, J., van Aardenne, J., Fischer, H., de Reus, M., Williams, J., and Winkler, P.: Increasing Ozone over the Atlantic Ocean, *Science*, 304, 1483–1487, doi:10.1126/science.1096777, 2004.

Meleux, F., Solmon, F., and Giorgi, F.: Increase in summer European ozone amounts due to climate change, *Atmos. Environ.*, 41, 7577–7587, doi:10.1016/j.atmosenv.2007.05.048, 2007.

Nakićenović, N., Alcamo, J., Davis, G., de Vries, B., Fenhann, J., Gaffin, S., Gregory, K., Grübler, A., Yong Jung, T., Kram, T., La Rovere, E. L., Michaelis, L., Mori, S., Morita, T., Pepper, W., Pitcher, H., Price, L., Riahi, K., Roehrl, A., Rogner, H.-H., Sankovski, A., Schlesinger, M., Shukla, P., Smith, S., Swart, R., van Rooijen, S., Victor, N., and Dadi, Z.: Emission scenarios, A special report of working group III of the Intergovernmental Panel on Climate Change, Cambridge University Press, 2000.

Parrish, D. D., Millet, D. B., and Goldstein, A. H.: Increasing ozone in marine boundary layer inflow at the west coasts of North America and Europe, *Atmos. Chem. Phys.*, 9, 1303–1323, doi:10.5194/acp-9-1303-2009, 2009.

Prather, M., Gauss, M., Bernsten, T., Isaksen, I., Sundet, J., Bey, I., Brasseur, G., Dentener, F., Derwent, R., Stevenson, D., Grenfell, L., Hauglustaine, D., Horowitz, L., Jacob, D., Mickley, L., Lawrence, M., von Kuhlmann, R., Müller, J.-F., Pitari, G., Rogers, H., Johnson, M., Pyle, J., Law, K., van Weele, M., and Wild, O.: Fresh air in the 21st century?, *Geophys. Res. Lett.*, 30, 1100–1104, doi:10.1029/2002GL016285, 2003.

Robertson, L., Langner, J., and Engardt, M.: An Eulerian limited-area atmospheric transport model, *J. Appl. Meteorol.*, 38, 190–210, 1999.

## European summer surface ozone 1990–2100

J. Langner et al.

[Title Page](#)
[Abstract](#)
[Introduction](#)
[Conclusions](#)
[References](#)
[Tables](#)
[Figures](#)
[Back](#)
[Close](#)
[Full Screen / Esc](#)
[Printer-friendly Version](#)
[Interactive Discussion](#)


Roeckner, E., Brokopf, R., Esch, M., Giogietta, M., Hagemann, S., Kornblueh, L., Manzini, E., Schlese, U., and Schulzweida, U.: Sensitivity of simulated climate to horizontal and vertical resolutions in the ECHAM5 atmosphere model, *J. Climate*, 19, 3771–3791, doi:10.1175/JCLI3824.1, 2006.

5 Royal Society: Ground-level Ozone in the 21st Century: Future Trends, Impacts and Policy Implications, Science Policy Report 15/08, Royal Society, London, 2008.

Samuelsson, P., Jones, C. G., Willén, U., Ullerstig, A., Gollvik, S., Hansson, U., Jansson, C., Kjellström, E., Nikulin, G., and Wyser, K.: The Rossby Centre Regional Climate model RCA3: Model description and performance, *Tellus A*, 63, 4–23, doi:10.1111/j.1600-0870.2010.00478.x, 2011.

10 Simpson, D., Andersson-Sköld, Y., and Jenkin, M. E.: Updating the chemical scheme for the EMEP MSC-W oxidant model: Current status, EMEP MSC-W Note 2/93, Norwegian Meteorological Institute, Oslo, 1993.

15 Simpson, D., Guenther, A. Hewitt, C. N., and Steinbrecher, R.: Biogenic emissions in Europe: 1. Estimates and uncertainties, *J. Geophys. Res.*, 100, 22875–22890, doi:10.1029/95JD02368, 1995.

Thomson, A. M., Calvin, K. V., Smith, S. J., Kyle, G. P., Volke, A., Patel, P., Delgado-Arias, S., Bond-Lamberty, B., Wise, M. A., Clarke, L. E., and Edmonds, J. A.: RCP4.5: a pathway for stabilization of radiative forcing by 2100, *Climatic Change*, 109, 77–94, doi:10.1007/s10584-011-0151-4, 2011.

20 van Loon, M. R., Vautard, R., Schaap, M., Bergström, R., Bessagnet, B., Brandt, J., Builtjes, P. J. H., Christensen, J., Cuvelier, K., Graff, A., Jonson, J., Krol, M., Langner, J., Roberts, P., Rouil, L., Stern, R., Tarrasón, L., Thunis, P., Vignati, E., White, L., and Wind, P.: Evaluation of long-term ozone simulations from seven regional air quality models and their ensemble, *Atmos. Environ.*, 41, 2083–2097, doi:10.1016/j.atmosenv.2006.10.073, 2007.

25 Wild, O., Fiore, A. M., Shindell, D. T., Doherty, R. M., Collins, W. J., Dentener, F. J., Schultz, M. G., Gong, S., MacKenzie, I. A., Zeng, G., Hess, P., Duncan, B. N., Bergmann, D. J., Szopa, S., Jonson, J. E., Keating, T. J., and Zuber, A.: Modelling future changes in surface ozone: a parameterized approach, *Atmos. Chem. Phys.*, 12, 2037–2054, doi:10.5194/acp-12-2037-2012, 2012.

## European summer surface ozone 1990–2100

J. Langner et al.

**Table 1.** Modelled surface O<sub>3</sub> compared to observed values over the years 1990–2009 at EBAS stations in Europe<sup>a</sup>.

	Observation ppbv	Model ppbv	bias %	spatial correlation	RMSE ppbv	#stations
Apr–Sep mean						
North of 50° N	31.8	33.8	6.3	0.06	4.8	45
South of 50° N	37.8	38.1	0.9	0.58	5.2	49
Apr–Sep mean of daily max						
North of 50° N	42.4	41.4	–2.3	0.61	3.4	45
South of 50° N	52.1	48.6	–6.6	0.58	5.3	49

<sup>a</sup> Modelled (Increasing boundary case, ECH\_RCP4.5\_BCtrend) and measured average values at EBAS sites were constructed for years with measurement data capture exceeding 75 % to account for trend in emissions and observed trend in hemispheric background. Sites at an elevation deviating more than 250 m from the model height were excluded from the evaluation. Model data were taken from the level 3 m above surface.

[Title Page](#)
[Abstract](#)
[Introduction](#)
[Conclusions](#)
[References](#)
[Tables](#)
[Figures](#)
[Back](#)
[Close](#)
[Full Screen / Esc](#)
[Printer-friendly Version](#)
[Interactive Discussion](#)


## European summer surface ozone 1990–2100

J. Langner et al.

Title Page

Abstract

Introduction

Conclusions

References

Tables

Figures

◀

▶

◀

▶

Back

Close

Full Screen / Esc

Printer-friendly Version

Interactive Discussion



**Table 2.** Model simulated surface O<sub>3</sub> mean, trend and variability<sup>a</sup> during different periods, averaged over the European land area.

	Apr–Sep daily max				Apr–Sep mean			
	1990–2009	2040–2059	2080–2099	1990–2099	1990–2009	2040–2059	2080–2099	1990–2100
	ppbv		ppbv century <sup>-1</sup>		ppbv		ppbv century <sup>-1</sup>	
North of 50° N								
ECH_RCP2000_BC2000	40	39	39	–0.5	32	32	32	–0.5
HAD_RCP2000_BC2000	42	41	41	–0.8	33	33	33	–0.8
ECH_RCP4.5_BC2000	40	34	32	–9.2	32	28	26	–7.2
ECH_RCP4.5_BCtrend	40	36	35	–5.0	32	30	29	–3.8
South of 50° N								
ECH_RCP2000_BC2000	50	51	53	3.5	38	39	40	2.1
HAD_RCP2000_BC2000	51	52	54	3.2	39	40	40	1.9
ECH_RCP4.5_BC2000	50	41	38	–12.8	39	32	30	–9.5
ECH_RCP4.5_BCtrend	50	43	41	–9.7	38	33	32	–7.1
variability ppbv								
North of 50° N								
ECH_RCP2000_BC2000	1.9	2.2	2.7		1.7	1.5	2.1	
HAD_RCP2000_BC2000	1.8	2.6	1.9		1.4	2.0	1.5	
ECH_RCP4.5_BC2000	3.3	2.2	1.6		2.4	1.8	1.3	
ECH_RCP4.5_BCtrend	3.0	1.7	1.8		2.1	1.6	1.5	
South of 50° N								
ECH_RCP2000_BC2000	2.4	4.3	6.2		1.4	2.3	3.5	
HAD_RCP2000_BC2000	2.9	6.0	5.3		1.6	3.3	2.9	
ECH_RCP4.5_BC2000	5.7	3.7	4.2		3.2	2.5	3.0	
ECH_RCP4.5_BCtrend	5.2	3.7	4.5		2.8	2.4	3.2	

<sup>a</sup> Variability is defined as the difference between the highest and lowest summer mean value in each 20-yr period. Trends are linear and calculated from 1990 to 2100.

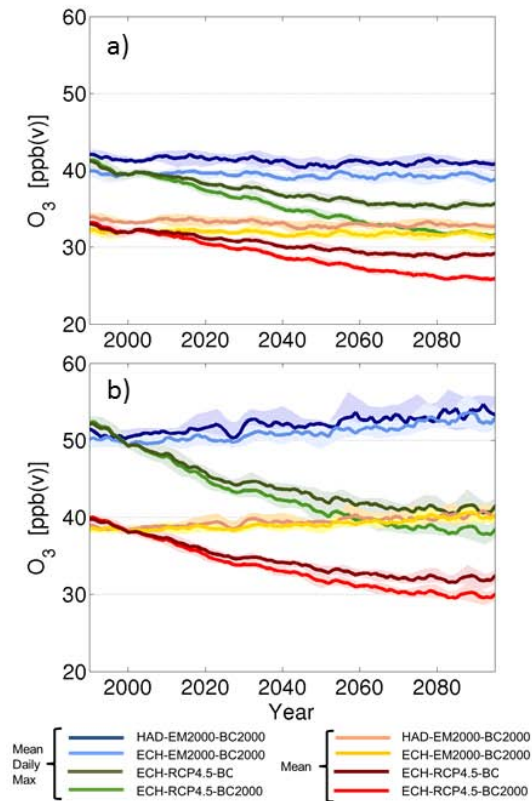


**Fig. 1.** Simulated geographical-average evolution of summer (April–September) mean surface  $O_3$  concentration and summer mean of daily maximum surface  $O_3$  concentration from 1990 to 2100. Results are **(a)** for the European land area north of  $50^\circ N$  and **(b)** south of  $50^\circ N$ . Thick lines correspond to a 5-yr running mean and the shaded areas correspond to the interval between the 5-yr running mean of the minimum and maximum summer mean values.

**European summer surface ozone 1990–2100**

J. Langner et al.

Title Page

Abstract Introduction

Conclusions References

Tables Figures

◀ ▶

◀ ▶

Back Close

Full Screen / Esc

Printer-friendly Version

Interactive Discussion



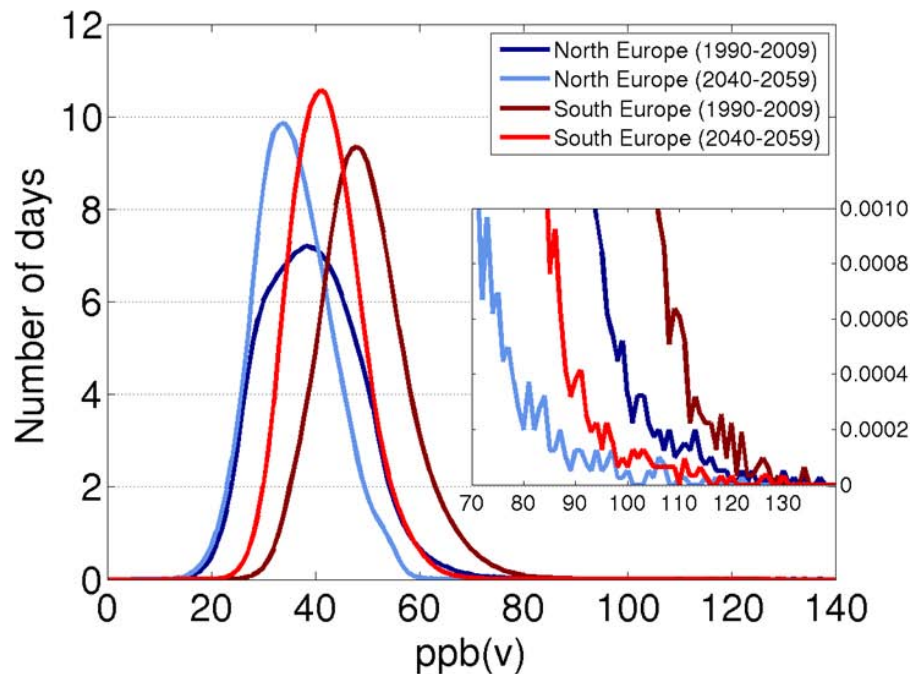


**Fig. 2.** Frequency distributions of daily max  $O_3$  concentrations in North and South Europe during the periods 1990–2009 and 2040–2059 in the Increasing boundary case simulation. The distributions show the number of days per year one arbitrary model grid point in northern and southern Europe experiences daily maximum  $O_3$  concentrations between  $X$  and  $X + 1$  ppbv during the respective 20-yr period.

**European summer surface ozone 1990–2100**

J. Langner et al.

Title Page

Abstract Introduction

Conclusions References

Tables Figures

◀ ▶

◀ ▶

Back Close

Full Screen / Esc

Printer-friendly Version

Interactive Discussion



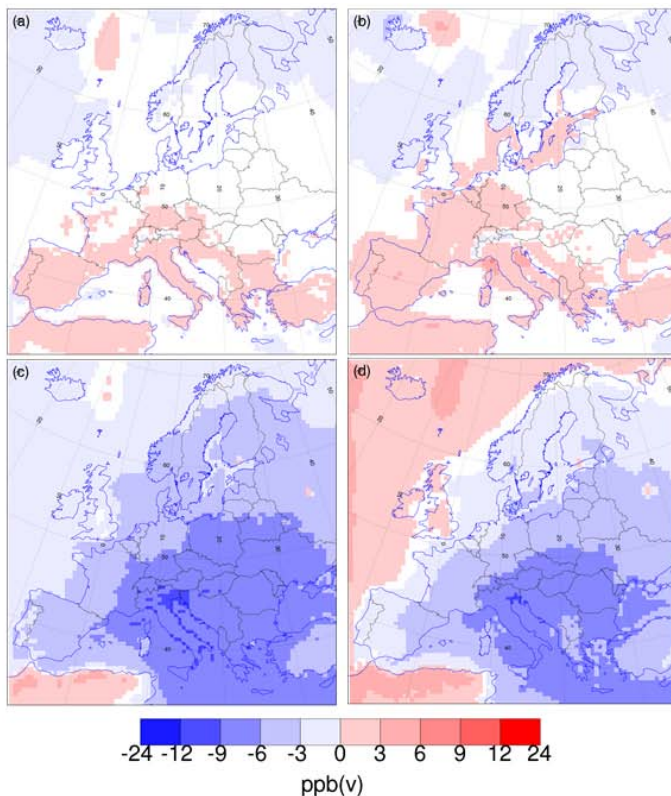


**Fig. 3.** Change in summer (April–September) mean surface  $O_3$  concentration from 1990–2009 to 2040–2059. **(a)** and **(b)** changes due to change in climate only; RCA3 downscaling of ECHAM5 and HadCM3, respectively. **(c)** ECHAM5 downscaling and change in European  $O_3$  precursor emissions. **(d)** Increasing boundary case; the combined change due to change in climate, change in  $O_3$  precursor emissions and an increasing hemispheric background of  $O_3$  of  $0.1 \text{ ppbv yr}^{-1}$ . Non-significant changes at 95 % confidence level are masked white.

**European summer surface ozone 1990–2100**

J. Langner et al.

Title Page	
Abstract	Introduction
Conclusions	References
Tables	Figures
◀	▶
◀	▶
Back	Close
Full Screen / Esc	
Printer-friendly Version	
Interactive Discussion	



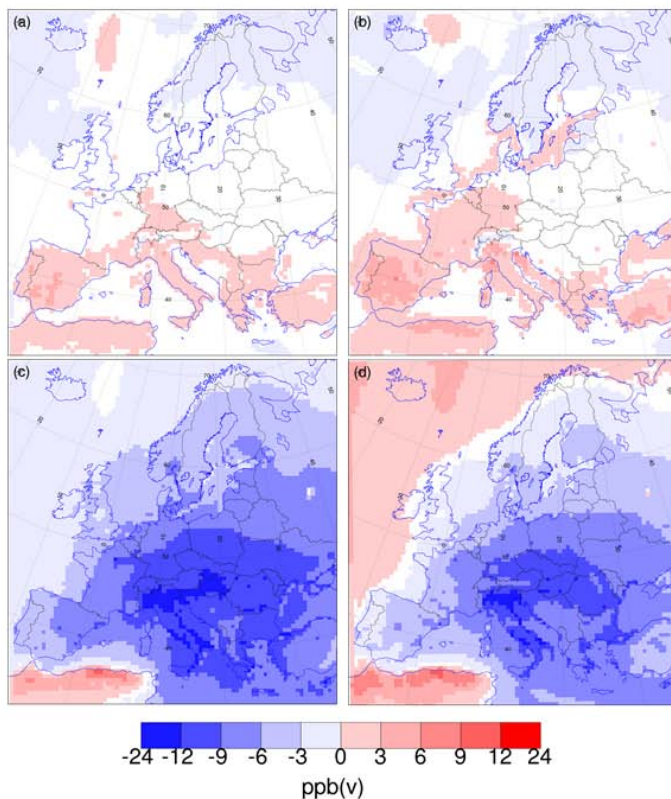


**Fig. 4.** Change in summer (April–September), daily maximum, surface O<sub>3</sub> concentration from 1990–2009 to 2040–2059. **(a)** and **(b)** changes due to change in climate only; RCA3 downscaling of ECHAM5 and HadCM3, respectively. **(c)** ECHAM5 downscaling and change in European O<sub>3</sub> precursor emissions. **(d)** Increasing boundary case; the change due to combined change in climate, change in O<sub>3</sub> precursor emissions and an increasing hemispheric background of O<sub>3</sub> of 0.1 ppbv yr<sup>-1</sup>. Non-significant changes at 95 % confidence level are masked white.